SYNTHESIS AND ELECTROCHEMICAL BEHAVIOR OF $LiFePO_4$/C WITH AIR-ELECTRODE FOR AQUEOUS LITHIUM ION BATTERY

NURHASWANI BINTI ALIAS

UNIVERSITI SAINS MALAYSIA

MARCH 2015

SYNTHESIS AND ELECTROCHEMICAL BEHAVIOR OF $LiFePO_4$/C WITH AIR-ELECTRODE FOR AQUEOUS LITHIUM ION BATTERY

by

NURHASWANI BINTI ALIAS

Thesis submitted in fulfillment of the requirements

for the degree of

Master of Science

March 2015

DECLARATION

I hereby declare that I have conducted, completed the research work and written the dissertation entitled: "Synthesis and Electrochemical Behavior of $LiFePO_4$/C with Air-Electrode for Aqueous Lithium Ion Battery". I also declare that it has not been previously submitted for the award of any degree or diploma or other similar title of this for any other examining body or University.

Name of student: Nurhaswani Binti Alias Signature :

Date : 02.03.2015

Witnessed by

Supervisor: Assoc. Prof. Dr Ahmad Azmin Bin Mohamad Signature :

Date : 02.03.2015

ACKNOWLEDGEMENTS

All praise to Allah, the Most Beneficent and Most Merciful, for giving me the strength to successfully complete this thesis. I also thank my supervisor, Assoc. Prof. Dr. Ahmad Azmin Mohamad, for his valuable support, technical guidance, and understanding throughout the course of this research. I further thank the Universiti Sains Malaysia (USM) for its financial support through the USM Fellowship Scheme and Postgraduate Research *Grant* Scheme (PRGS*)*. I acknowledge as well the Ministry of Higher Education through the MyBrain15 sponsorship.

I express my sincere appreciation to all academic and technical staff of the School of Materials and Mineral Resources Engineering, USM for their contributions to and assistance during my studies. I also thank my fellow colleagues in the research team for their continuous support and for providing stimulating discussions and ideas. Finally, I thank my lovely mother, Noriah Binti Mahmud and beloved family for their love, strength, understanding, and inspiration that enabled me to complete this thesis. My deepest gratitude is to my late father, Alias Bin Mohamed Kassim, who is my greatest supporter. His advice and guidance will always remain in my heart forever.

NURHASWANI BINTI ALIAS

March 2015

TABLE OF CONTENTS

CHAPTER 4: RESULTS AND DISCUSSION

LIST OF TABLES

LIST OF FIGURES

LIST OF ABBREVIATIONS

ARLB	Aqueous Rechargeable Lithium ion Battery
AB	Acetylene Black
BET	Brunauer, Emmet and Teller
BJH	Barret, Joyner and Halenda
CD	Charge Discharge
CE	Counter Electrode
CV	Cyclic Voltammetry
DSC	Differential Scanning Calorimetry
EDX	Energy Dispersive X-Ray
FESEM	Field Emission Scanning Electron Microscopy
GoF	Good of Fitness
HRTEM	High Resolution Transmission Electron Microscopy
ICSD	Inorganic Crystal Structure Database
Ni-Cd	Nickel-cadmium
Ni-MH	Nickel-metal hydride
Pb-acid	Lead-acid
RE	Reference Electrode
SCE	Saturated Calomel Electrode
TGA	Thermal Gravimetric Analysis
TEM	Transmission Electron Microscopy
WE	Working Electrode
XRD	X-ray Diffraction

LIST OF SYMBOLS

%	Percentage
<	Less than
>	More than
°	Degree
Ω	Ohm
λ	Wave length
wt. %	Weight percent
$cm^2 sec^{-1}$	Centimeter square per second
$S cm^{-1}$	Siemen per centimeter
$mA h g^{-1}$	Mili-ampere hour per gram
$Wh kg^{-1}$	Watt hour per kilogram
°C	Degree Celsius
$°C min^{-1}$	Degree Celsius per minute
A	Ampere
C	Current rate
cm	Centimeter
nm	Nanometer
eV	Electron volt
g	Gram
h	Hour
Hz	Hertz
K	Kelvin

Li^+	Lithium ions
R_{ct}	Charge transfer resistance
R_s	Electrolyte resistance
R_{wp}	Weight R profile
V	Voltage
V_{OCP}	Open circuit voltage

LIST OF CHEMICAL FORMULAS

EC/DEC	Ethylene carbonate-diethyl carbonate
ED/DMC	Ethylene carbonate-dimethyl carbonate
Fe_2P	Iron phosphide
H_2	Hydrogen
H_2O	Water
$LiCoO_2$	Lithium cobalt oxide
$LiFePO_4$	Lithium iron phosphate
$LiFePO_4/C$	Lithium iron phosphate carbon coated
$LiMn_2O_4$	Lithium manganese oxide
$LiNO_3$	Lithium nitrate
LiOH	Lithium hydroxide
Li_2SO_4	Lithium sulphate
Li_3PO_4	Trilithium phosphate
LiV_3O_8	Lithium vanadium oxide
N_2	Nitrogen
O_2	Oxygen
Pt	Platinum
VO_2	Vanadium oxide

SINTESIS DAN TINGKAH LAKU ELEKTROKIMIA $LiFePO_4$/C DENGAN ELEKTROD-UDARA UNTUK BATERI AKUES LITIUM ION

ABSTRAK

Bateri akues litium ion bateri yang boleh dicas semula (ARLB) telah menjadi satu solusi yang bagus untuk mengatasi isu kos dan keselamatan yang ditimbulkan oleh bateri litium ion konvensional yang mengandungi elektrolit organik. Baru-baru ini, lapisan karbon telah dibuktikan mampu untuk mengelakkan kesan secara langsung diantara partikel nano dan persekitaran, termasuk O_2 dan H_2O. Ini membantu untuk mendapatkan bateri berkapasiti tinggi bersama penambah baikan bagi kapasiti penyimpanan dalam persekitaran akua. Asid sitrik melalui kaedah sol-gel telah digunakan dalam kajian ini untuk menyediakan litium ferum fosfat yang diselaputi karbon ($LiFePO_4$/C) dengan menggunakan suhu pengkalsinan yang berbeza (500-800 °C). Analisa struktur dan unsur mengesahkan bahawa sampel yang dikalsinasi merupakan hablur orthorombik $LiFePO_4$ yang dilapisi jumlah karbon yang berbeza. Morfologi dan hasil penyerapan fizikal menunjukkan struktur berliang daripada $LiFePO_4$/C dalam lingkungan liang meso. Suhu pengkalsinan mempengaruhi saiz kristalit, fasa bendasing, dan luas permukaan dan sampel $LiFePO_4$/C dalam system ARLB yang dikalsinasikan pada suhu 700 °C menawarkan ciri-ciri yang optimum. Ini disokong oleh tingkah laku elektrokimia $LiFePO_4$/C dalam akues bateri litium-ion yang disatukan bersama dengan elektrod-udara apabila $LiFePO_4$/C yang dikalsinasikan pada suhu 700 °C menunjukkan kitaran voltammetri dengan tindak balas yang tertinggi, kerintangan yang terendah (6.11 Ω) bersama kapasiti yang terbaik (83 mA h g^{-1} pada 1.0 C). Selain itu, kestabilan kitaran yang baik dicapai apabila sampel $LiFePO_4$/C berjaya mengekalkan kapasiti sekitar 90 mA

h g^{-1} selama 30 kitaran pada 0.5 C. Sebaliknya, $LiFePO_4$ yang terdedah dan dikalsinasikan menggunakan suhu yang sama (700 °C) mempamerkan prestasi elektrokimia yang rendah dengan kadar pemudaran kapasiti yang lebih tinggi (45 % bagi 30 kitaran pada 0.5 C) disebabkan oleh kerintangan yang tinggi (18.98 Ω). Kadar keupayaan sampel $LiFePO_4$/C yang dikalsinasikan pada suhu 700 °C juga dibandingkan dengan elektrod tambahan platinum; elektrod-udara menunjukkan tingkah laku kitaran yang lebih baik.

SYNTHESIS AND ELECTROCHEMICAL BEHAVIOR OF $LiFePO_4$/C WITH AIR-ELECTRODE FOR AQUEOUS LITHIUM ION BATTERY

ABSTRACT

An aqueous rechargeable lithium ion battery (ARLB) has become a great solution to overwhelm the cost and safety issue of the conventional lithium ion battery with organic electrolyte. Recently, the in situ carbon layer was proven to avoid any direct contact between the nanoparticles and the environment, including O_2 and H_2O. This help to achieve high capacity battery with improved capacity retention in aqueous environment. A citric acid assisted sol-gel method is employed in this study to prepare carbon-coated lithium iron phosphate ($LiFePO_4$/C) using different calcination temperatures (500–800 °C). The phase structure and elemental analyses confirmed the orthorhombic crystal structure of $LiFePO_4$ surrounded by different amounts of carbon layer. The morphologies and physical absorption results proved the porous structure of $LiFePO_4$/C with a mesoporous range. The calcination temperature influences the crystallite size, impurity phase, and surface area as the $LiFePO_4$/C calcined at 700 °C offered the optimum properties. This finding was supported by the electrochemical behavior of $LiFePO_4$/C in the ARLB system with an air-electrode. The $LiFePO_4$/C calcined at 700 °C showed the highest current response for cyclic voltammetry and the lowest impedance (6.11 Ω) with a good discharge capacity (83 mA h g^{-1} at 1.0 C). In addition, good cycling stability was achieved as the $LiFePO_4$/C maintained a discharge capacity of approximately 90 mA h g^{-1} within 30 cycles at 0.5 C. By contrast, bare $LiFePO_4$, which was calcined at the same calcination temperature (700 °C), exhibited poor electrochemical performance with high capacity fading (45 % within 30 cycles at 0.5 C) because of high

impedance (18.98 Ω). The rate capability of the $LiFePO_4$/C calcined at 700 °C was also compared with that of a platinum counter electrode; the air-electrode still showed better cycling behavior.

CHAPTER 1

INTRODUCTION

1.1 Background of the study

Lithium iron phosphate ($LiFePO_4$) was first suggested by Padhi et al. [1] about 20 years ago as a next-generation cathode material for rechargeable lithium ion (Li-ion) batteries. Since then, $LiFePO_4$ has received considerable attention because of its superior thermal stability, low toxicity, and low cost. However, the performance of $LiFePO_4$ is limited by its poor electronic conductivity and the sluggish kinetics of lithium (Li^+) ions to diffuse through the $LiFePO_4/FePO_4$ interface, which can result in a significant loss of capacity at high currents [2-4].

To introduce fast ionic and electronic paths into a battery cathode, the electrochemical behavior can be improved by increasing the porosity of $LiFePO_4$ particles [5, 6]. As the porosity increases, the surface area for electrolyte penetration is increased and the electrochemical performance of $LiFePO_4$ is enhanced. Adding a chelating agent to the $LiFePO_4$ synthesized by sol–gel method significantly improves porosity with a wide size distribution (1–200 nm) and an average value of approximately 50 nm after heating at 700 °C [7].

The degradation of the chelating agent produces a layer of carbon on the $LiFePO_4$ particle, which increases the conductivity of $LiFePO_4$ and controls the particle size by preventing it from agglomeration. Furthermore, the chelating agent

can contribute in keeping the Fe^{2+} oxidation state of the Fe ions in $LiFePO_4$ with improved electrochemical response [8, 9].

Rechargeable lithium ion battery with an aqueous electrolyte (ARLB) has attracted the attention of researchers because it offers low fabrication cost and increases the safety and environment awareness as compared with Li-ion batteries with organic electrolytes [10, 11]. In addition, the electrochemical performance of this battery has been proven to be better as compared with other aqueous batteries such as lead-acid (Pb-acid), nickel-cadmium (Ni-Cd), and nickel-metal hydride (Ni-MH) batteries because of its high energy density [12-14].

$LiFePO_4$ was first reported as a cathode material in ARLB system around 2006. The oxidation of $LiFePO_4$ to $FePO_4$ in LiOH electrolyte was found to be not fully reversible, which result in poor cycling behavior [15]. However, $LiFePO_4$ in aqueous electrolyte with high capacity of 140 mA h g^{-1} at current density of 1.0 C and good electrochemical behavior was reported later by Ping et al. [16]. The electrochemical improvement of $LiFePO_4$ in aqueous solution is attributed to the carbon layer that protects the $LiFePO_4$ from rapid capacity deterioration.

All of these remarkable electrochemical behaviors of the ARLB system show a big step toward improving the design of a high-safety, high-power, low-cost, and long-cycling life battery. These characteristic are suitable for high-power and stationary-power to store energy from sustainable sources such as turbine and solar energy systems.

1.2 Problem statement

Previous studies have reported on the excellent kinetics of the electrochemical insertion of Li^+ ions into $LiFePO_4$ in aqueous solution system. However, exposure of $LiFePO_4$ to oxygen or water results in Li loss and increase in number of Fe(III) ions [17]. A high capacity loss of 37 % was observed for pure $LiFePO_4$ after 10 cycles in aqueous environment [10].

Attempts have been made to improve the rate capabilities and capacity retentions of electrode materials in aqueous electrolyte using full carbon-coating technology [18, 19]. An improved capacity retention of carbon-coated material has been conveyed, amounting to 92 %–95 % after 80 cycles in an aqueous solution equilibrated with air [20]. In aqueous electrolyte, the carbon layer could reduce the dissolution of iron element into the electrolyte and suppress capacity fading. Therefore, good rate capability and high stability of $LiFePO_4$/C could be achieved in aqueous electrolyte.

The electrochemical performance of $LiFePO_4$/C in an aqueous electrolyte has been investigated previously using a simple three-electrode cell with lithium vanadium oxide (LiV_3O_8) as reversible counter electrode (CE) [21]. The results have shown that this cell system has excellent cycling behavior because the electrode displays good rate capability and can achieve a discharge capacity of 60 mA h g^{-1} at 50 C even after 500 cycles. From one point of view, the fundamental aspect to conduct the electrochemical characterization for three-electrode cell is the use of Li^+ ions reversible source as CE.

However, particular studies on suitable reversible CE are still limited. Oxygen (O_2) has been proven to be an efficient oxidizing agent that can be used to produce electrochemical energy for metal-air batteries, such as zinc-air, aluminum-air, and lithium-air batteries [22-24]. Inexhaustible O_2 from the air can be directly reduced using an air-electrode to deliver capacity. Furthermore, the O_2 reduction product is solubilized in aqueous solution [25]. Therefore, a study on the ability of oxygen as a reversible CE should be considered for the ARLB system.

1.3 Objectives of the study

The objectives of this study are:

i. To determine the effect of calcination temperature on $LiFePO_4$/C synthesis using sol–gel method

ii. To determine the effect of chelating agent on $LiFePO_4$/C synthesis using sol–gel method

iii. To determine the effect of $LiFePO_4$/C with different CE on the electrochemical performance of ARLB

1.4 Thesis outlines

This chapter presents an introduction to the thesis with a brief explanation on the problems and the objectives of the present study. Chapter 2 reviews the introduction of Li-ion battery and ARLB as well as some basic concepts regarding the mechanism of Li^+ ions with significant existing literature studies. A comparison between the ARLB and conventional Li-ion batteries are elucidated closely. In addition, the pioneer of $LiFePO_4$ as cathode materials in ARLB is discussed as well as their structure, properties, and synthesis technique. Further information are given on the factors that influence the electrochemical properties of $LiFePO_4$/C in the ARLB, including the effects of calcination temperature, chelating agent, and CE on the ARLB system.

Chapter 3 explains the methodologies used in this work, including the synthesis of the material ($LiFePO_4$/C and bare $LiFePO_4$), fabrication of ARLB, and the experimental setup. All results of these studies are presented in Chapter 4. The thermal, structural, morphological, and physisorption properties are discussed for further understanding. Apart from that, the electrochemical results comprising cyclic voltammetry (CV), impedance, charge–discharge (CD) capacity, and cycle life are exhibited as well. Finally, Chapter 5 summarizes the whole thesis with conclusions and future works as recommendations.

CHAPTER 2

LITERATURE REVIEW

2.1 Introduction

This chapter provides a review of previous studies related to this research. It is divided into three sections as follows:

(i) Development of lithium ion (Li-ion) as rechargeable battery including basic concepts

(ii) Development of aqueous rechargeable lithium ion battery (ARLB) including principles and advantages of aqueous electrolyte as compared with organic electrolyte in Li-ion batteries

(iii) Pioneering of $LiFePO_4$ as cathode materials in ARLB, as well as the structures and properties of these materials, synthesis technique, and factors that influence the electrochemical performance of $LiFePO_4$/C in ARLB

2.2 Development of Li-ion rechargeable battery

A rechargeable battery system is an energy storage that can be continuously discharged and charged over a long period of time [26]. Rechargeable batteries have been conceptualized since 1859, when the lead acid (Pb-acid) battery was first developed by Plante [27]. Since then, rapid advancement of battery technology has reported with the introduction of nickel-cadmium (Ni-Cd), nickel–metal hydride (Ni-MH), and Li-ion batteries as tabulated in Table 2.1. These rechargeable batteries have used different chemical systems to generate electricity [26, 28]

Concern on the limited availability of energy resources and environmental pollution has increased the demand for renewable energies (including solar, wind, and tidal energies), and at the same time, development of energy storage systems with high power and energy density [29-31]. As alternative energy supply for portable equipment, consumer electronic devices, and high-power applications, such as electric vehicles and power storage for renewable energy, rechargeable Li-ion batteries have become predominant power sources and are the most feasible option, owing to their superior performances, flexibility in design, and excellent energy density [32-34].

Table 2.1: Various types of rechargeable battery technologies at cellular level [26, 28]

Technology	Electrolyte	Nominal voltage (V)	Cell reaction	Costs (€/ kWh)
Lead acid	H_2SO_4 (4-6 M)	2.0	C : $PbO_2 + 4H^+ + SO_4^{2-} + 2e^- \leftrightarrow PbSO_4 + 2H_2O$ A : $Pb + SO_4^{2-} \leftrightarrow PbSO_4 + 2e^-$ O : $PbO_2 + 2H_2SO_4 + Pb \leftrightarrow 2PbSO_4 + 2H_2O$	25-40 (OEM) 100-180 (After market)
Nickel cadmium	KOH (4.5-7 M)	1.2	C : $2NiOOH + 2H_2O + 2e^- \leftrightarrow 2Ni(OH)_2 + 2OH^-$ A : $Cd + 2OH- \leftrightarrow Cd(OH)_2 + 2e^-$ O : $2NiOOH + Cd + 2H_2O \leftrightarrow Ni(OH)_2 + Cd(OH)_2$	200-500 (OEM)
Nickel metal hydride	KOH (4.5-7 M)	1.2	C : $Ni(OH)_2 + OH^- \leftrightarrow NiO(OH) + H_2O + e^-$ A : $M + e^- + H2O \leftrightarrow MH + OH^-$ O : $M + Ni(OH)_2 \leftrightarrow MH + NiO(OH)$	275- 550 (OEM) 600 (HEV)
Lithium ion ($LiFePO_4$)	Organic electrolyte + Li salt	3.4	C : $Li_{1-x}FePO_4 + {}_xLi^+ + xe^- \leftrightarrow LiFePO_4$ A : $Li_xC_6 \leftrightarrow {}_xLi^+ + 6C + {}_xe^-$ O : $Li_xC_6 + Li_{1-x}FePO_4 \leftrightarrow LiFePO_4 + 6C$	200-500 (OEM) 400-800 (HEV)

OEM: original equipment manufacturer; HEV: hybrid electric vehicle

Due to the high energy capacity, long lifetime, and light weight of Li-ion battery, it has become the most powerful energy storage among rechargeable batteries [35, 36]. For example, Pb-acid batteries, which are mostly used in automobile applications, cannot be considered potential energy storage for high-power applications because of low energy density, although these batteries are inexpensive. Rapid degradation of Ni-MH batteries also hinders their utilization for large-scale energy storage [12, 14]. In addition, environmental concerns have also caused the gradual decline of Ni-Cd and Pb-acid batteries in the market, as cadmium and lead are poisonous elements [37].

2.2.1 Li-ion battery: Basic concept and principle

A rechargeable Li-ion battery consists of a positive electrode (cathode) which is an electron acceptor generally a lithium metal oxide (e.g., $LiFePO_4$), and a negative electrode (anode), an electron donor such as graphite (Figure 2.1). Usually, a separator physically splits the anode and cathode in the electrolyte, thereby allowing movement of ions instead of electrons. The working principle of rechargeable Li-ion batteries is based on the electro-insertion reaction called intercalation process [38]. Li-ion batteries are also known as "rocking-chair batteries" because Li^+ ions move between the anode and cathode through the electrolyte during the charge and discharge (CD) process.

During the charging process, the positive Li^+ ions travel from the cathode to the electrolyte and intercalate between the carbon layers in the graphite anode. Simultaneously, electrons migrate through the external circuit from the cathode to

the anode. The cathode compensates the removal of Li^+ by oxidizing the transition metal present in the lattice (Fe^{+2} to Fe^{+3}) without major structural changes. A reverse process also occurs in the discharge process, as the Li^+ ions move out of the graphite through the electrolyte and back to the cathode. Iron is subsequently reduced (Fe^{+3} to Fe^{+2}) and forms $LiFePO_4$. External electric current is also used to supply power to the electronic devices. This process occurs repeatedly, and the chemical reaction in this electrode is described as follows.

$$LiFePO_4 + C_6 \leftrightarrow Li_xC_6 + Li_{1-x}FePO_4 \quad (2.1)$$

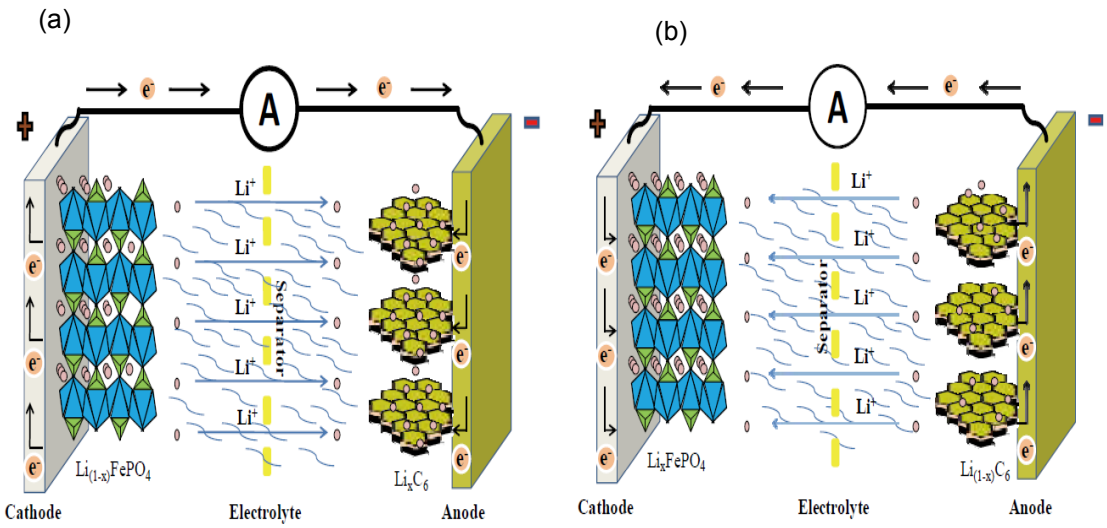

Figure 2.1: Schematic of Li-ion battery for (a) charging and (b) discharging process [38]

Cell capacity is generally expressed as the total quantity of electricity involved in an electrochemical reaction and defined in coulombs or ampere-hours [26]. The ampere-hour capacity of a battery is directly associated with the quantity of electricity obtained from the active materials. Based on Faraday's first law, the mass

of a substance deposited, dissolved, or evolved at an electrode is proportional to the quantity of electrical charge passed during electrolysis. The theoretical capacity, Q_s can be calculated from the equation below:

$$Q_s = \frac{n\ x\ F}{M} \tag{2.2}$$

where n is the number of moles of electrons transferred in the electrochemical reactions, F is the Faraday constant (96, 487 C), and M is the molecular weight of the active materials. Specific charge–discharge capacities (Q_c or Q_d) are calculated as follows:

$$Q_C \text{ or } Q_d = \frac{I\ x\ t}{m} \tag{2.3}$$

where I is the current (A), t is the time (h), and m is the mass of the material (kg).

The battery rate capability is also determined by the ability to deliver a large capacity when discharged at high C rates. A rate of C/1 corresponds to the current required to completely discharge an electrode within 1 h. C denotes either the theoretical charge capacity or the nominal capacity of the battery. The coulombic efficiency (η) of a battery is also important to determine the charge–discharge efficiency of a cycle. The η can be calculated by the ratio of the amount of charge that enters the battery during charging and the amount that can be extracted from the battery during discharging. The coulombic efficiency is calculated as follows:

$$\eta = \frac{n^{th} Q_c}{n^{th} Q_d} x\ 100\ \% \quad (2.4)$$

2.3 Development of ARLB

The ARLB systems are based on water. An aqueous solution is an ideal electrolyte solvent because of its nature, abundance, and total environmental friendliness. Moreover, most secondary batteries use water-based electrolytes (Table 2.1 excluding the lithium ion system). However, considering the working mechanisms of these commercially available secondary batteries with aqueous electrolytes (Pb-acid, Ni-Cd, and Ni-MH), none could provide long cycling stability compared with Li-ion batteries that use organic electrolytes.

Despite the superior performance of organic Li-ion batteries, fabrication cost and safety concerns have limited the use of large-scale energy storage systems. Beck and Ruetschi [35] highlighted the "Three E" criteria, namely, energy (high energy content with respect to unit weight and volume), economics (low manufacturing costs and long cycling life), and environment (safety, non-toxicity, and high reliability), to determine the suitable energy storage system for applications. Hence, the use of aqueous electrolytes has been recommended as a promising approach because water-based battery systems require low cost and provide high safety.

In the mid-1990s, Dahn et al. [39] proposed the ARLB to replace the flammable organic solvent with a green and safe aqueous electrolyte. This system yields an average operating voltage of 1.5 V with energy (75 Wh kg^{-1}) larger than that of Pb-acid batteries (30 Wh kg^{-1}). The redox behavior of Li-ion batteries with

aqueous electrolytes shows a similar mechanism in organic Li-ion batteries. The "rocking chair" concept is successfully applied when Li^+ ions intercalate into/from the host in the aqueous media. To date, many ARLB systems have been investigated, and improvement in the cycling behavior has been well reported (Table 2.2) [10, 11, 16, 18, 20, 21, 40-46].

2.3.1 ARLB: Principles of electrochemical performance

The foundation of the ARLB system is related to the intercalation of Li^+ ions in an aqueous environment. To allow the reversible reaction of Li^+ ions into/from the host of electrode materials in water, the intercalation potential range of the electrode should lie within the electrochemical stability windows of the aqueous electrolyte. Considering the ARLB can be fabricated using two different intercalation compounds (with different chemical potentials by several eVs), a suitable material for the intercalation of Li^+ ions should be selected to avoid water decomposition [47, 48].

The electrochemical stability window of pure water is about 1.23 V. However, this stability limit can be expanded because of the kinetic effect [49]. For instance, Pb-acid [50] and aluminum–air batteries [51] undergo wide potential stability windows of electrolytes compared with that of pure water (>1.23 V). The potential of the intercalation compound and stability limit of water as a function of pH (ranging from 0 to 14) is illustrated in the Pourbaix diagram shown in Figure 2.2.

Table 2.2: Cell performance of various rechargeable Li-ion battery systems

Cathode	**Anode**	**Electrolyte**	**Capacity retention (%) (per cycles)**	**Current density (mA g^{-1})**	**Capacity (mA h g^{-1})**	**Ref.**
$LiFePO_4$	Activated carbon	Li_2SO_4 (0.5 M)	63 % (10)	5.0 C	124	[10]
$LiFePO_4$	Activated carbon	Li_2SO_4 (0.5 M)	45 %	20.0 C	58	[16]
$LiFePO_4$ /C	LiV_3O_8	$LiNO_3$ (9.0 M)	99 % (100)	10.0 C	90	[21]
$LiFePO_4$	$LiTi_2(PO_4)_3$	Li_2SO_4 (1.0 M)	90 % (1000)	6.0 C	55	[40]
$LiFePO_4$ /C	VO_2	$LiNO_3$ (Saturated)	94 % (50)	C/3	106	[20]
$LiMn_2O_4$	VO_2	$LiNO_3$ (Saturated)	83 % (42)	0.2 C	120	[41]
$LiMn_2O_4$	Activated carbon	Li_2SO_4 (0.5 M)	93 % (10,000)	90.0 C	118	[42]
$LiMn_2O_4$	TiP_2O_7	$LiNO_3$ (5.0 M)	85 % (10)	0.2 C	42	[43]
$LiMn_2O_4$	Activated carbon	Li_2SO_4 (0.5 M)	99 % (200)	4.5 C	110	[44]
$LiMn_2O_4$	Activated carbon	Li_2SO_4 (0.5 M)	94 % (1200)	4.5 C	110	[45]
$LiCoO_2$	Ppy	Li_2SO_4 (Saturated)	63 % (120)	0.1 C	104	[46]

The electrode with an intercalation potential ranging from 3 V to 4 V vs. Li^+/Li can be used as the cathode electrode for the ARLB (before O_2 evolution). For example, the Li^+ ions will be intercalated into the $Li_{1-x}Mn_2O_4$ and be reduced during discharge. The $LiMn_2O_4$ immersed in 1 M LiOH undergoes the following reaction [52]:

$$Li_{1-x}Mn_2O_4 + xLi^+ + xOH^- \rightarrow LiMn_2O_4 + (x/2)H_2O + (x/4)O_2 \quad (2.5)$$

This reaction is expected based on the position of $Li_{1-x}Mn_2O_4$ relative to water at pH 14. The anode, which is the intercalated carbon placed in water, will undergo the following reaction [52]:

$$Li_xC_6 + xH_2O \rightarrow C_6 + xLi^+ + xOH^- + (x/2)H_2 \quad (2.6)$$

The "rocking chair" concept, similar to the conventional Li-ion battery with organic electrolytes, is also demonstrated in the ARLB system by Mi et al. [49]. Figure 2.3 shows the cyclic voltammogram of $LiFePO_4$ electrodes in both aqueous (1 M Li_2SO_4) and organic [1 M $LiPF_6$-EC/DMC (1:1)] electrolytes. A well reversible redox reaction of $LiFePO_4$ electrodes in both systems has demonstrated parallel mechanisms for Li^+ ion intercalations.

In the non-aqueous $LiPF_6$-EC/DMC electrolyte (Figure 2.3a), the prepared $LiFePO_4$ electrode (with a scan rate of 0.2 mV s^{-1}) displayed only a couple of broad peaks at about 2.90 V to 3.30 V vs. Li^+/Li (reduction) and 3.70 V to 3.90 V vs. Li^+/Li (oxidation) (Figure 2.3a). The corresponding voltage scale vs. saturated calomel electrode (SCE) also showed redox peaks noticed at −0.142 V vs. SCE (reduction) and 0.558 V vs. SCE (oxidation),

respectively. This finding corresponds to the two-phase CD reactions of the Fe^{3+}/Fe^{2+} redox couple.

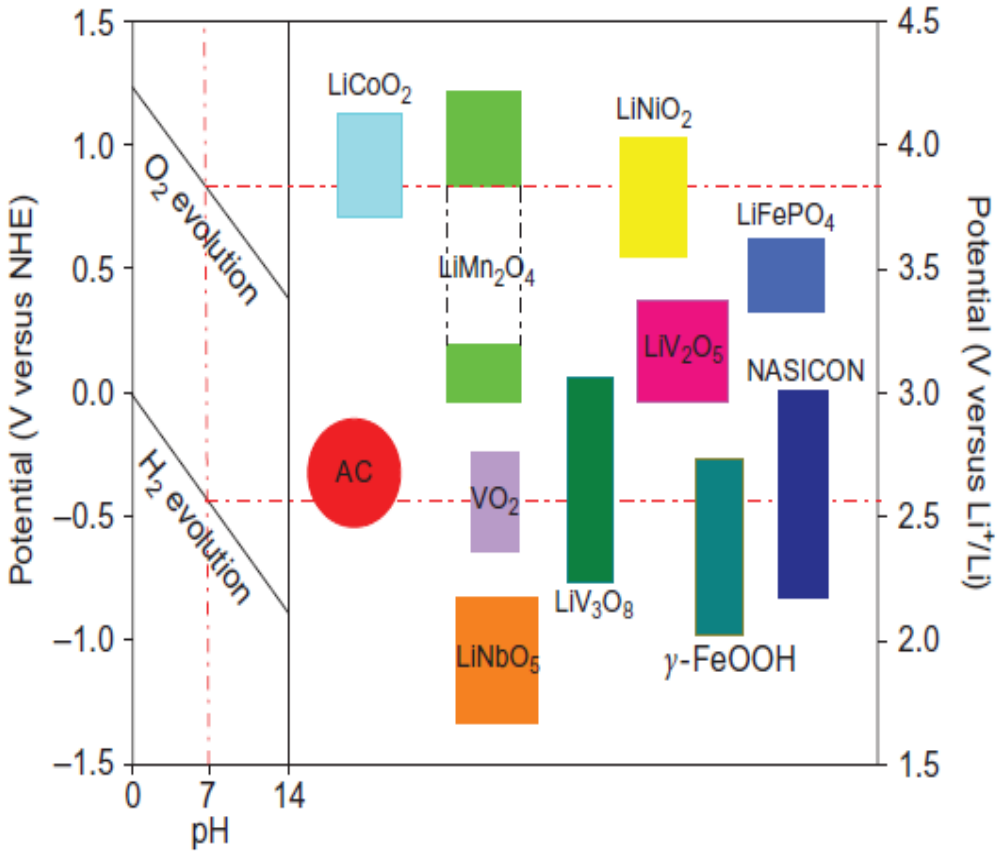

Figure 2.2: Stability potential window for intercalation/de-intercalation of Li^+ ions for selected compound vs. Li metal (left) and vs. NHE (right) in aqueous solution [40]

For the $LiFePO_4$ electrodes in 1 M Li_2SO_4 aqueous solution (Figure 2.3b), the redox peaks appeared at −0.270 (reduction) and 0.495 V vs. SCE (oxidation) at scan rate of 1 mV s^{-1}. The redox process occurred in the safe potential window of electrolytes without H_2O decomposition. The initial potentials of O_2 and H_2 evolutions were about 1.2 and 0.9 V vs. SCE, respectively. These findings indicated the expansion of the stability limit for aqueous solution to >1.23 V (stability window of pure water). Therefore, both systems undergo extraction and intercalation of Li^+ ions during the charge–discharge process.

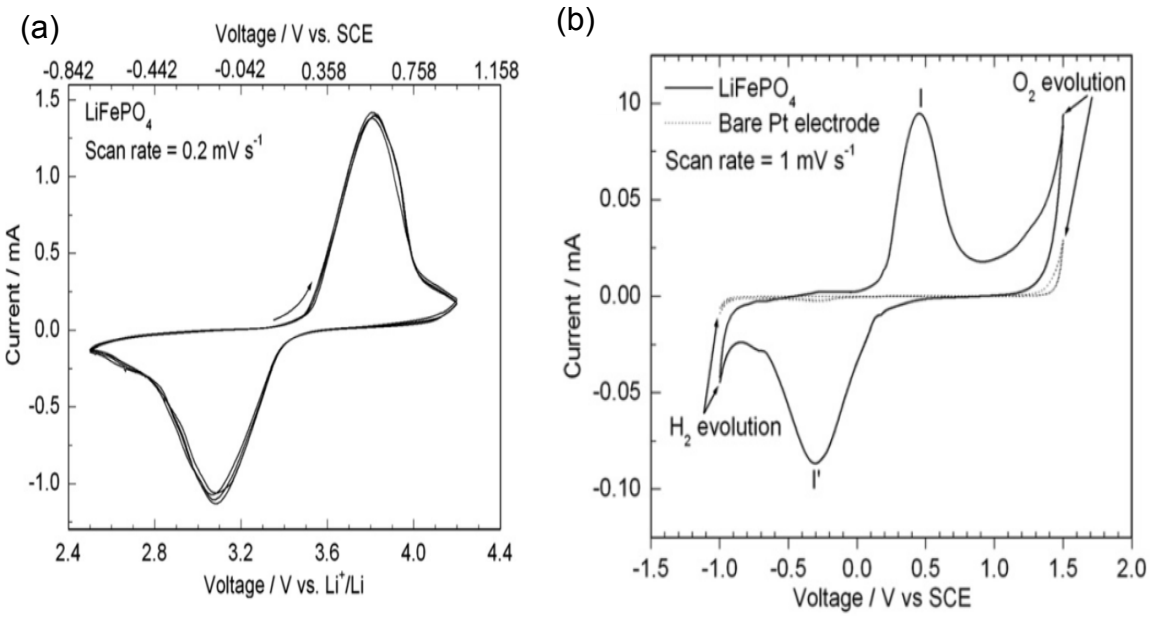

Figure 2.3: Cyclic voltammograms of $LiFePO_4$ electrode in (a) 1 M $LiPF_6$-EC/DMC (1:1) non-aqueous electrolyte and (b) 1 M Li_2SO_4 aqueous electrolyte [49]

2.3.2 ARLB: Comparison between aqueous and organic electrolytes

Batteries consist of three important components, namely, cathode, anode, and electrolyte. The electrolyte is used as an ionic conductor to provide medium for ions to transfer between the anode and cathode phases [26]. The ions in the electrolyte should diffuse in the system with high mobility to completely utilize the active material [53]. Despite the excellent performance of the Li-ion batteries with organic electrolytes, ARLB is a better choice for low-cost energy and safety.

For commercial Li-ion batteries, the high price of organic electrolytes and separators influences the cost of battery manufacturing. Thus, Li-ion batteries become overpriced, particularly for high power demands. The high price is also influenced by the cost of materials and the fabrication process, which accounts for 80 % to 90 % of the total costs of high-power and high-energy batteries [54]. The strict fabrication process of the Li-

ion batteries with organic electrolytes also requires a glove box that can avoid moisture from reacting with the organic solvent. Thus, more cost is added.

Developers are currently seeking ways to decrease maintenance and operating costs, while simultaneously producing batteries that can deliver high power and good efficiency. With the presence of an aqueous solution as electrolyte, the cost of Li-ion battery fabrication can be effectively reduced by:

i. Replacement of expensive Li salts, such as $LiPF_6$, with cheap ones including $LiNO_3$, LiOH, and Li_2SO_4;
ii. Replacement of expensive separator with a cheap one suitable for aqueous electrolytes; and
iii. Elimination of the glove box (in the production line), given that the ARLB can be fabricated in an open system.

On the other hand, the use of aqueous electrolytes for Li-ion batteries has been a good solution to the safety problem of such batteries with organic electrolytes. As listed by Wang et al. [55], numerous fires and explosions involving Li-ion batteries in mobile phones and electrical vehicles have been reported worldwide, and most cases are caused by thermal runaways. Aqueous electrolytes exhibit high thermal capacitance and can absorb large amount of heat [56]. Therefore, the temperature of the system using aqueous electrolytes will be much lower than that of commercial Li-ion batteries during the charge–discharge process. A good cooling effect is also achieved as the aqueous electrolytes are in direct contact with both the anode and cathode electrodes. Thus, an additional cooling system will not be needed for high-capacity battery modules.

Aqueous electrolytes also exhibit advantages in terms of high ionic conductivity and good-rate capability. The ionic conductivity of aqueous electrolytes is two orders of magnitude higher than that of some organic electrolytes, resulting in low electrolyte impedance and high discharge rate (fast charge transfer kinetics) [57]. As a result, the cell resistant value of the aqueous system will be lower than that of the organic solution, even if both have the same concentration [26, 58]. The high ionic conductivity of the electrolyte is very important for achieving high rate capability and good reversibility in batteries.

Given that the aqueous electrolytes exhibit higher ionic conductivity, the ARLB system can be fabricated using thicker electrodes. The thicker electrode helps to reduce the fabrication cost as high capacity battery can be fabricated since the mass of active material increase. However, other aspect such as the resistance effect for a thick electrode should be considered as well to fabricate this high rate and high capacity battery.

From the above discussion, the ARLB is characterized by the following:

(i) Good safety as no explosion will occur in water-based electrolytes;

(ii) Environmental friendliness (water is safe and abundant);

(iii) Low fabrication cost (cheap and good availability of Li salts or separators);

(iv) Easy fabrication as no strict control is needed to control humidity;

(v) High ionic conductivity (suitable for charging and discharging at a high rate); and

(vi) Excellent cycling behavior.

2.4 $LiFePO_4$ as a cathode material of ARLB

To date, several cathode material candidates have been reported for the ARLB system, such as $LiFePO_4$, $LiMn_2O_4$, and $LiCoO_2$ as shown previously in Table 2.2. Ever since its discovery by Padhi [1] in 1997, $LiFePO_4$ has been the most extensively studied cathode materials due to its excellent thermal stability, flat voltage profile (170 A h kg^{-1} at a V_{oc} = 3.45 V vs. Li/Li^+), and long-term cyclability. $LiFePO_4$ also exhibits low material cost, abundant material supply, and better environmental compatibility.

By contrast, $LiCoO_2$ and $LiMn_2O_4$ materials face the crucial problem of high cost and adverse electrochemical effects, as these cathodes commonly include rare metals of the redox center [59]. The severe fading of $LiMn_2O_4$ caused by Jahn–Teller distortion and the unusual valence state of Co^{4+} on fully charged $LiCoO_2$ are also factors of concern with regard to chemical stability of these materials.

2.4.1 $LiFePO_4$: Structure and properties

The $LiFePO_4$ belongs to the olivine family of lithium orthophosphate. The structure of $LiFePO_4$ consists of corner-shared FeO_6 octahedrons (b-c plane, forming zigzag planes), edge-shared LiO_6 octahedrons running parallel to the b-axis, and PO_4 groups which share one edge with a FeO_6 octahedron and two edges with LiO_6 octahedrons (Figure 2.4). Li and Fe are located at octahedral sites, whereas P is located at tetrahedral sites with distorted hexagonal close-packed framework [60, 61]. Both LiO_6 and FeO_6 run parallel to the *c*-axis and alternately in the *b* direction. The *a–c* planes containing the Li atoms are bridged by the PO_4 tetrahedron. The Li^+ ions diffuse along the *b*-axis in the crystal of

orthorhombic $LiFePO_4$ with a space group of *Pnma* during the charge–discharge process [62-64].

The structure of $LiFePO_4$ is stable and suitable for charge–discharge cycles because it is quite similar to that of $FePO_4$ [3, 65]. With extraction of Li^+ ions from the host of $LiFePO_4$, the volume decreases by only 6.81 % [3]. The small change in volume will avoid severe capacity degradation that can cause by large volumetric changes during the intercalation process. This finding explains well the excellent electrochemical cyclability of $LiFePO_4$ in the Li-ion battery system.

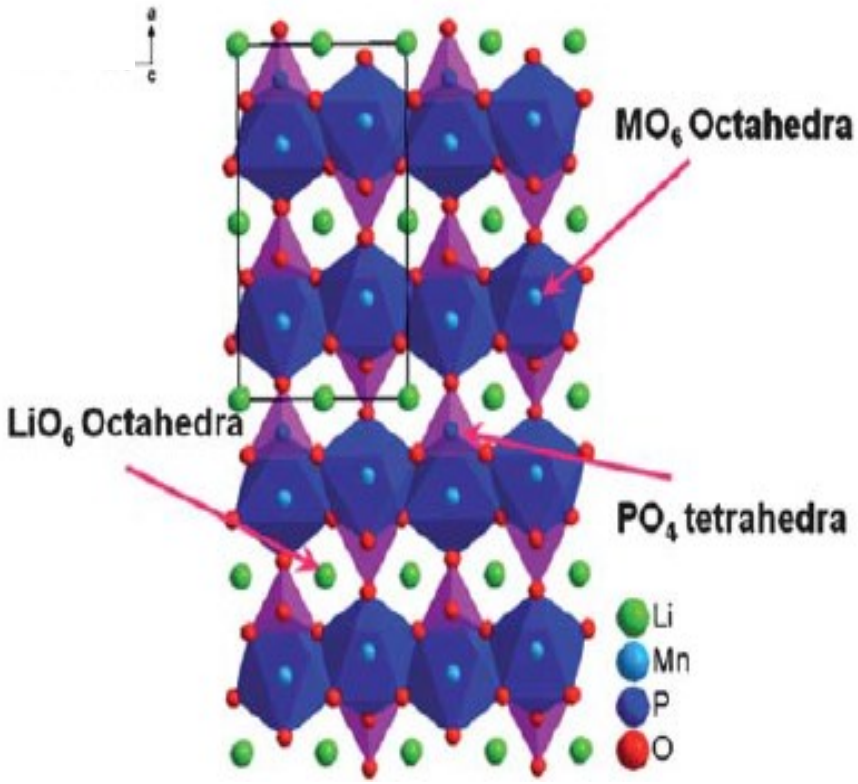

Figure 2.4: Crystal structure of $LiFePO_4$ [60]

The crystal structure of $LiFePO_4$ is also suitable for intercalation of Li^+ ions in aqueous environment. Given that the ARLB system involves aqueous solutions, other cations, such as the proton (H^+), may be co-intercalated into the electrode materials parallel to the intercalation of Li^+ ions. However, the H^+ insertion does not occur for olivine $Li_{1-x}FePO_4$ crystal structure, whereas delithiated layered $Li_{1-x}CoO_2$ and $Li_{1-x}Ni_{1/3}Mn_{1/3}Co_{1/3}O_2$ show a significant concentration of H^+ in the lattice during deep Li^+ extraction [19, 66].

The large distortion of the Fe and P coordination polyhedron that must be severely distressed for the structure to accommodate H^+ causes the unfavorable H^+ insertion into the olivine structure. Further investigations were conducted by Benedek et al. [67] who reported a solid explication regarding the free energy of the protonation reaction in Li-ion battery cathode materials. Based on their first-principle calculations, three types of crystal structure were clarified for protonation behavior. The H^+ insertion is:

i. most favorable in the layered structure (Li_2MnO_3 and $LiCoO_2$);
ii. less favorable in the spinel structure ($LiMn_2O_4$ and LiV_3O_8); and
iii. unfavorable in the olivine structure ($LiFePO_4$).

On the other hand, the stability of $LiFePO_4$ cathode material is attributed to the strong P–O covalent bonding, which is thermodynamically stable and can withstand very high temperatures, thereby improving safety [68]. This finding was supported by Jiang et al. [69] who reported the thermal stability of three different cathode materials, namely, $LiCoO_2$, $Li(Ni_{0.1}Co_{0.8}Mn_{0.1})O_2$, and $LiFePO_4$ in organic solvent ethylene carbonate/diethyl carbonate (EC/DEC); $LiFePO_4$ shows higher stability than other materials. Moreover, the high lattice stability results in excellent cyclic performance of $LiFePO_4$.

However, the strong covalent oxygen bonds also lead to low ionic diffusivity (10^{-13} cm^2 s^{-1} to 10^{-16} cm^2 s^{-1}) and poor electronic conductivity (~10^{-9} S cm^{-1}) [70, 71]. As a result, only ~60 % to 70 % of the capacity could be obtained from the original $LiFePO_4$, and its capacity decreases with increased current density. Therefore, an appropriate synthesis method should be developed to obtain highly pure $LiFePO_4$ and improve the conductivity properties.

2.4.2 $LiFePO_4$: Sol-gel method

Designing materials with proper composition, morphology, and microstructure are crucial to obtain batteries with excellent electrochemical performance [72, 73]. Good properties of electrode materials, such as high surface area, high conductivity, and short distance path of Li^+ ions, are very important for achieving better Li^+ ion intercalation and outstanding electrochemical behavior. These properties of electrode materials can be controlled by synthesis method.

The $LiFePO_4$ can be synthesized using several synthesis routes including the solid-state synthesis [74, 75], hydrothermal synthesis [76-78], co-precipitation [79, 80] and sol-gel method [81-85]. The $LiFePO_4$ has been first synthesized using conventional solid-state method [1]. However, the uncontrollable particle growth and agglomeration by the solid-state method have resulted in non-pure final materials with limited surface area and unsatisfactory particle-size distribution [86, 87].

By contrast, sol–gel method can modify the size and morphology of $LiFePO_4$ powders to produce high purity, fine uniformity, and small particle size with homogeneous distribution, good stoichiometric control, and in situ carbon coating, thereby forming $LiFePO_4$/C [38]. Son et al. [87] reported that the $LiFePO_4$ material obtained by sol–gel route composed of small particles (50 nm to 100 nm), which are smaller than those obtained by solid-state route (200 nm to 400 nm) as depicted in Figure 2.5.

Different morphologies of $LiFePO_4$/C synthesis by sol–gel and solid-state methods have also been revealed by Dominko et al. [86]; the $LiFePO_4$/C particles prepared by solid-state reaction show no pores on the surface, whereas pores of various magnitudes are easily found on the particles prepared by sol–gel method (Figure 2.6). The morphology affects the electrochemical performance of a material as better capacity (150 mA h g^{-1} at 0.1 C) is achieved for $LiFePO_4$/C synthesis by sol–gel compared with solid-state method (130 mA h g^{-1} at 0.1 C).

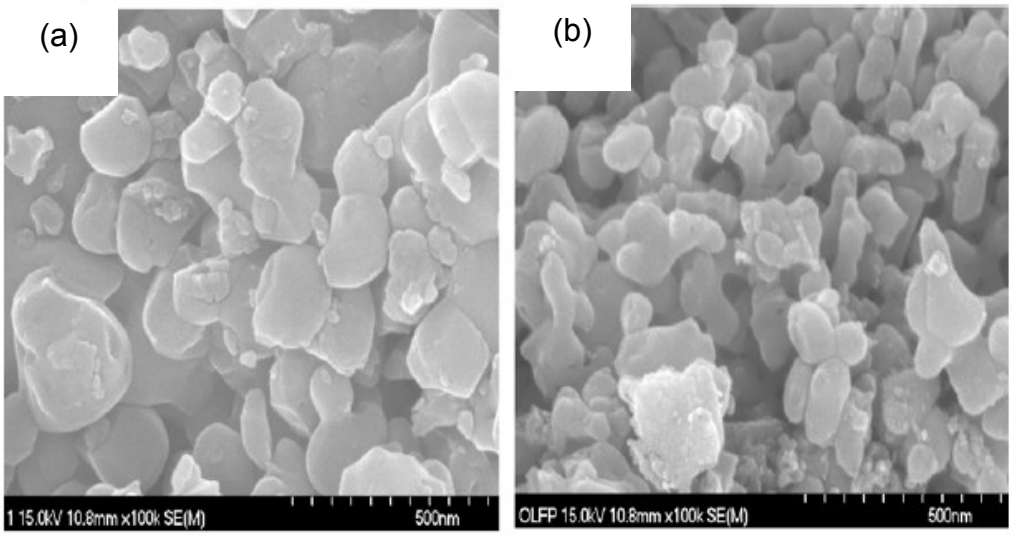

Figure 2.5: FESEM images of $LiFePO_4$ obtained by (a) solid-state method and (b) sol–gel method [87]

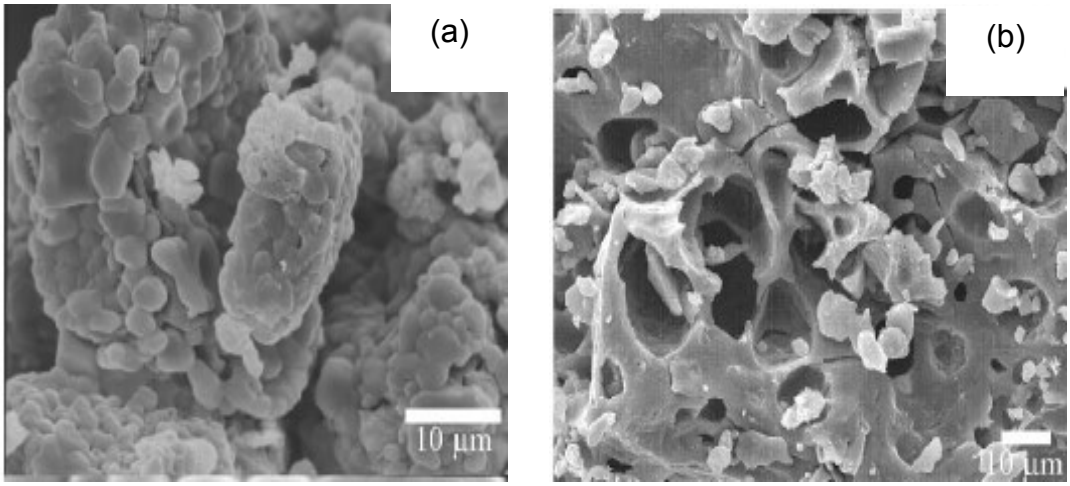

Figure 2.6: SEM images of $LiFePO_4/C$ composites prepared by (a) solid-state technique and (b) sol–gel technique at heating rate of 5 K min^{-1} [86]

The different morphologies of $LiFePO_4/C$ synthesis by sol–gel method may be ascribed to the reaction parameters, including precursor selection, heat treatment, and ratio of the chelating agent, which influenced the formation of the obtained powder [38]. For example, the morphology of $LiFePO_4/C$ using different ions (other than citrate based) was reported to create nanoparticles other than micro- or nanoporous materials [88]. However, the mechanism leading to different morphologies remains unclear.

To date, different precursors and chelating agents have been used in sol–gel synthesis to produce $LiFePO_4/C$ powders as shown in Table 2.3 [8, 83, 87, 89-94]. For sol–gel method, reaction parameters, such as carbon source [89, 95-97], doping [90], calcination time [84], and calcination temperature [81], were studied in detail to improve the formation of $LiFePO_4$, as well as the particle size and shape, pore size, and surface area. These approaches have also been reported to enhance the electrical conductivity of $LiFePO_4/C$ powder and increase the electrochemical behavior of Li^+ intercalation.